PRAMANA
— journal of
physics

Vol. 41, No. 5,
November 1993
pp. 429–442

Magnetic properties of ultra-fine particles of $Mn_{0.5}Fe_{0.5}Fe_2O_4$ spinel system

R V UPADHYAY and R V MEHTA
Department of Physics, Bhavnagar University, Bhavnagar 364002, India

MS received 12 July 1993

Abstract. A systematic study of the magnetic properties of ultra-fine particles of $Mn_{0.5}Fe_{0.5}Fe_2O_4$ spinel system has been undertaken. The effect of temperature on the magnetic properties of particles and the ferrofluid has been studied. Analysis of the data yields information on the anisotropy constant, particle size distribution and superparamagnetic behaviour. The results are explained on the basis of existing theories.

Keywords. Magnetic properties; ferrofluid; particles

PACS Nos 75·50; 75·60

1. Introduction

Study of transition metal oxides having a spinel structure is of much interest because of their remarkable electrical and magnetic properties [1–3]. These properties depend upon the type of magnetic ions residing on the tetrahedral (A) site and octahedral (B) site of the spinel lattice and the relative strength of the inter- and intra-sublattice interactions. This so-called cation distribution depends upon the preparation conditions [4–8]. It is well-known that the magnetic properties of ferrites depend upon the crystallite size of particles, because the properties of fine particles are drastically different from the bulk. This opens up an area of research that is very challenging scientifically as well as technologically. Fine particles are widely used for magnetic recording media, magnetic fluids (ferrofluids), catalysts, medical diagnostics, drug delivery systems and pigments in paints and ceramics [9–12]. Ultra-fine particles are single domain with diameter typically of the order of 100 A–150 A. For such particles, if the thermal energy (kT, where k is a Boltzmann constant and T the absolute temperature) is comparable to the magnetic anisotropy energy (KV, K = anisotropy constant, V = volume of the particle), the magnetic moment of the particle can relax during the measuring time which in turn, gives rise to a net zero magnetization in the absence of an applied magnetic field. Thus, an assembly of such particles exhibits superparamagnetic behaviour, i.e., zero remanence and coercivity [13]. In a real system of fine particles there exists a distribution of particle sizes. Therefore, in the magnetic properties of fine particles, the size distribution affects much, because of the relatively large surface to volume ratio.

In this paper we report a study of the ultra-fine ferrite particles of $Mn_{0.5}Fe_{0.5}Fe_2O_4$ (MF5) spinel system. The choice of this system is because of: (i) high value of domain magnetization (M_d) of $MnFe_2O_4$ (560 emu/cc) compared to Fe_3O_4 (510 emu/cc) at 0 K [1], (ii) the magnetocrystalline anisotropy (K_1) of $MnFe_2O_4$ ($0{\cdot}4 * 10^5$ erg/cc) is

much lower than Fe_3O_4 ($1{\cdot}1 * 10^6$erg/cc) at room temperature [14], (iii) low Curie temperature of $MnFe_2O_4$ (573 K compared to 858 K of Fe_3O_4) [1]. These properties are useful for preparation of ferro-fluid or magnetic fluid and their related applications.

A magnetic fluid consists of ultra-fine ferro-ferri-magnetic particles colloidally dispersed in a carrier liquid. Under the influence of an external magnetic field, such a fluid exhibits certain novel phenomena and several of its physical properties are modified [15–17]. The most commonly used magnetic material in ferrofluid at present is iron oxide, like magnetite, maghemite, etc. Many new engineering devices like rotating shaft seals, ferrofluid dampers, sensors, etc. are developed using ferrofluids [18–22]. But all these devices have different requirements for the properties of fluids. For example, in ink-jet printer for a character recognition, a ferrofluid involving particles of high remanence is required, while in rotating shaft seals, one prefers particles with low magnetocrystalline anisotropies. For some applications where movement of the fluid around a close loop is required, one needs fluid which has a large change in magnetization with a small change in temperature, i.e., low Curie temperature with large M_s. This property is the basis of an energy conversion system [23]. Therefore it is very important to know, before carrying out any fine particle preparation for magnetic fluid, for what exact application one needs this particles. Here our aim is to prepare a fluid with high saturation magnetization and low viscosity, which may be suitable for rotary shaft seals. Recently we have synthesized a stable magnetic fluid using 10% Mn substitution in Fe_3O_4 and studied its rheological properties [24]. This paper reports a detailed study of 50% Mn substituted Fe_3O_4 system.

2. Experimental details

2.1 *Preparation of fine particles and fluid*

Generally, a large number of techniques were used to prepare magnetic fine particles, like chemical reduction, sputtering, aersol synthesis, etc. [25–30], but here we have used a standard co-precipitation technique to produce fine particles of $Mn_{0{\cdot}5}Fe_{0{\cdot}5}Fe_2O_4$ system. The GPR grades, $FeCl_3 6H_2O$, $MnSO_4 4H_2O$ and $FeSO_4 7H_2O$ were used to obtain Fe^{3+}, Mn^{2+} and Fe^{2+} ions in an aqueous solution. These salts were mixed in required molar ratio in distilled water and added to 8M NaOH solution with constant stirring at room temperature. The precipitate was heated to 80°C with constant stirring and pH was maintained at 10·5. Aliquots of the reaction mixture was collected and washed with distilled water many times. Finally, the precipitate was washed with acetone and dried in air. The composition was checked by atomic absorption spectrometer. The result is given in table 1. The particles were coated with oleic acid and heated to 95°C for 5 min. In order to coagulate the oleic acid coated particles an acidic solution was added. After decantation, the product was washed with distilled water and acetone. This acetone wet slurry was dispersed in ISOPAR-M carrier and acetone was removed by warming the solution. The resulting fluid was found to be stable. The dispersion was liquid at room temperature and solid below 200 K.

2.2 *Structural characterization*

X-ray powder diffraction pattern was recorded on a Philips PW1130/90 X-ray diffractometer using CuKα radiation ($\lambda = 1{\cdot}5414$ A). The average particle size (D_xA)

Magnetic properties

Table 1. Characteristics properties of $Mn_{0.5}Fe_{0.5}Fe_2O_4$ system. D_e, D_x and D_m are electron microscopy, X-ray and magnetic particle size, respectively.

Chemical Analysis	: Fe/Mn (Cal)	Ratio 5	(Obs)	4·99
Structural Analysis				
a(Å)	: 8·445			
D_x(Å)	: 70			
D_e(Å)	: 69			
D_m(Å)	: 69			
σ_e	: 0·32			
σ_m	: 0·46			
Magnetic properties	: n_B(Bohr magneton)			
300 K	: 2·6			
4·2 K	: 3·3			

was calculated using Scherrer's formula, using the full width at half maximum intensity of the plane (311) of the pattern. The specimen was also examined using an AEI Cornith Transmission Electron Microscope (TEM).

2.3 *Magnetization measurements*

Room temperature magnetization measurements were carried out using a vibrating sample magnetometer (VSM). Low temperature measurements were performed using Oxford Instruments CF1200 cryostat. The magnetometer was calibrated using a nickel standard. DC-susceptibility measurement for fluid was carried out after the sample was cooled in zero field (i.e. randomly oriented anisotropy axes) and then warmed in presence of a small magnetic field ($H = 15$ Oe). The temperature decay of remanence (of fluid) was performed after the sample was cooled to 4·2 K in zero field. A saturating field of 10 kOe was applied, after setting the field to zero the remanence magnetization (M_r) was measured after 100 s. This procedure was repeated for each temperature.

2.4 *AC-susceptibility measurements*

The temperature dependence of the ac-susceptibility was measured between 80 K and 300 K using the technique described in [31]. The induced voltage was measured with both decreasing and increasing temperature for which no detectable hysteresis was measured (because the ac-susceptibility technique does not detect the irreversible component of magnetization).

2.5 *Mössbauer measurements*

Mössbauer measurements were carried out using a constant acceleration Mössbauer spectrometer with ^{57}Co source. Magnetic field was applied perpendicular to the direction of gamma ray propogation.

3. Results and discussion

3.1 *Microstructure analysis*

Figure 1 shows the X-ray diffraction pattern of MF5 with Miller indices (*hkl*). The structure of the powder prepared was definitely confirmed as isostructural with spinel i.e. cubic with space group F*d*3*m*. It is known [32] that if a sufficient amount of Mn^{3+} ion is present in the B-site, a tetragonally deformed ferrite coexists with the cubic spinel structure. In the present case no such peaks were observed, indicating the complete transformation of hydroxide into the spinel ferrite which is further confirmed by the atomic absorption technique, (table 1). In table 1 structure parameter, $a(A)$, and particle size, $D_x(A)$ are given. In comparison with magnetite, the value of $a(A)$ is greater. This observed increase can be explained by considering the ionic size effect. Because larger Mn^{2+} ion (0·81 A) replaces the smaller Fe^{3+} ion (0·63 A) from A-site, resulting in increase in $a(A)$. Considering the site preference energies of the constitutent ions [33] the cation distribution can be written as,

$$(Mn^{2+}_{0\cdot5}Fe^{3+}_{0\cdot5})^{A}[Fe^{2+}_{0\cdot5}+Fe^{3+}_{1\cdot5}]^{B}O^{2-}_{4}. \tag{1}$$

Figure 2 shows the electron micrograph for the MF5. The particle size and distribution parameters were obtained using Carl-Zeiss particle size analyser and method of O'Grady *et al* [34]. The line through the data points in figure 3 corresponds to the log-normal distribution best fit to the data given by,

$$F(D)dD=(1/\sigma D\sqrt{2\pi})*\exp[-\{\ln(D/D_0)\}^2/(2\sigma^2)]dD \tag{2}$$

where, $F(D)$ is the frequency function, D is the diameter of the particle, D_0 is the median physical diameter of the particle, σ is the standard deviation of $\ln(D/D_0)$. The parameters obtained are given in table 1. The result is in good agreement with the particle size determined from X-ray diffraction.

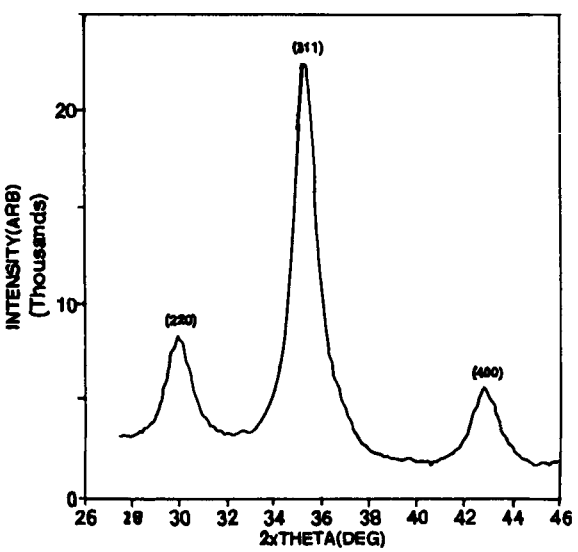

Figure 1. X-ray diffractogram pattern of MF5 fine particles.

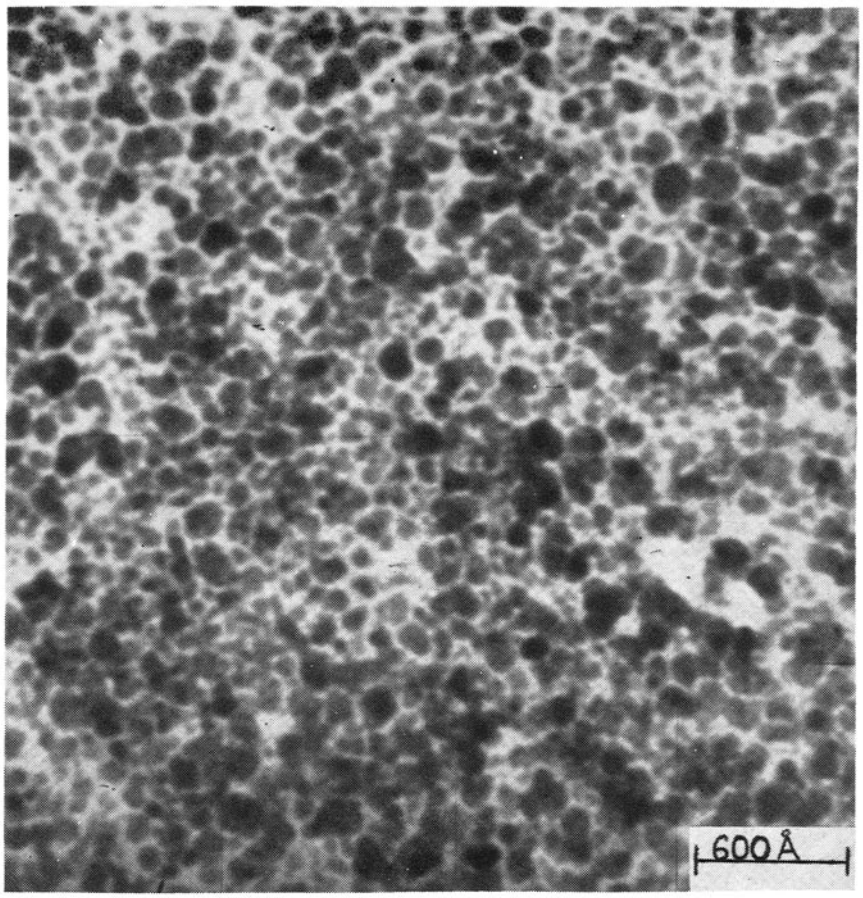

Figure 2. Electron micrograph of MF5 system.

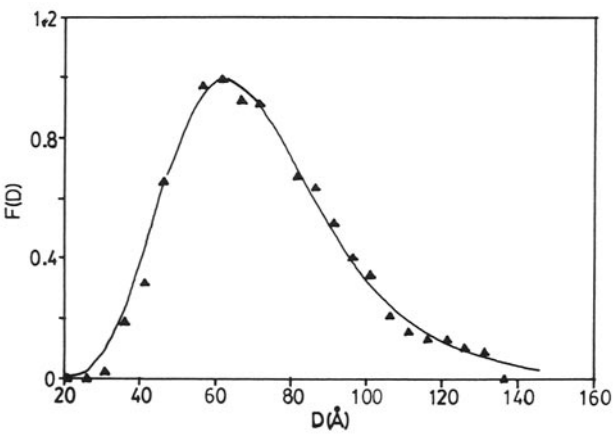

Figure 3. Particle size distribution determined from figure 2. The line corresponds to best fit of equation (2).

3.2 *Magnetic properties of particles*

Using the value of saturation magnetization, M_s, obtained from the M versus $1/H$ curve, the magnetic moment per formula unit, n_B, in Bohr magneton was calculated (table 1). Figure 4 shows the variation of saturation magnetization with temperature. The M_s value at 0 K was obtained by extrapolating the curve of M versus T at 0 K, and n_B was calculated. This n_B value is much lower than that calculated using (1). Therefore, the observed low value of magnetic moment cannot simply be explained by considering the cation distribution. It is evident from the X-ray and electron microscopy results that the particle size of ~ 70 A. Therefore one possibility of low M_s or n_B may be due to decrease in particle size. As the particle size decreases, the percentage of the atoms on the surface of the particle increases, as a result of this there are large number of spins which are uncoupled on the surface, i.e., spin pinning effect. Hence n_B decreases. The observed low value of Curie temperature also supports the concept of weakened spin coupling in the disordered surface layer. Inset in figure 4 shows the reduced magnetization variation with reduced temperature. The line through the data points is a line derived from Weiss–Langevin theory of ferromagnetism for the classical case, i.e. $J = \infty$. The low field data show that the particles have zero remanence and coercivity, indicating that the system is superparamagnetic at the time scale of measurement (100 s). In order to get further insight into this Mössbauer study was carried out.

Figure 5a shows the room temperature Mössbauer spectrum of the particles. The observed relaxation behaviour is explained as follows. It is known that [35] when particle size reduces below 200 A the magnetic anisotropy energy (KV) may become comparable to the thermal energy (kT) as a result the phenomena of fluctuation of direction of the magnetization commences. If we consider a particle with uniaxial anisotropy and with the magnetic energy given by the expression:

$$E(\theta) = KV\sin^2(\theta) \tag{3}$$

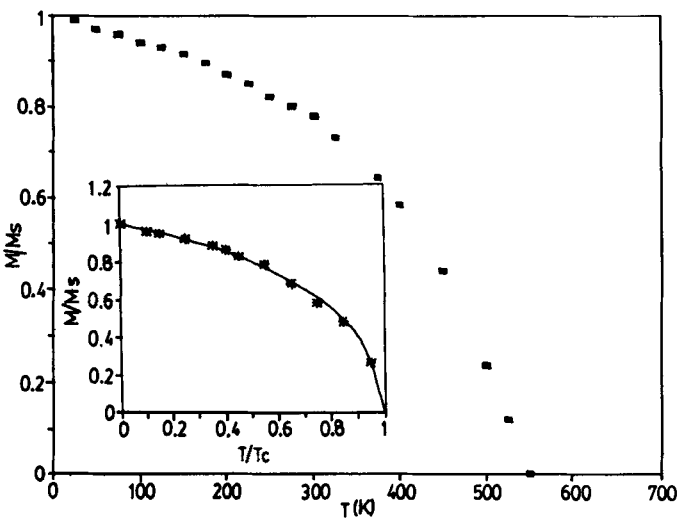

Figure 4. Temperature variation of magnetization for uncoated particles. Inset: Reduced magnetization versus reduced temperature, line is the classical case i.e. $J = \infty$ (see text).

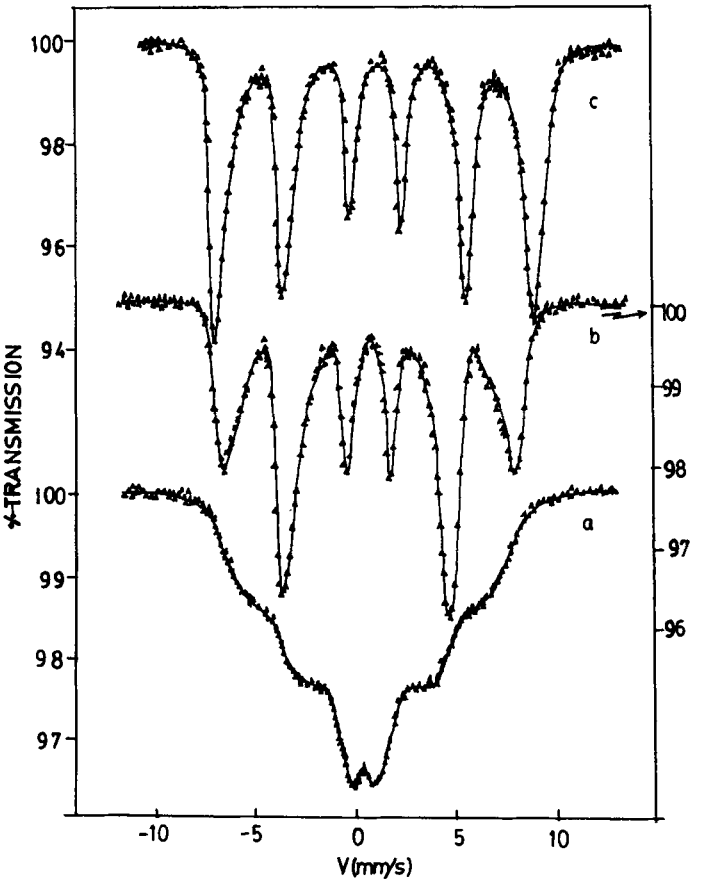

Figure 5. Mössbauer spectra of uncoated particles. (a) $T = 298$ K, $H = 0$ kOe. (b) $T = 298$ K, $H = 6$ kOe, (c) $T = 80$ K, $H = 0$ kOe.

where θ is the angle between the magnetization direction and an easy direction of magnetization, there are two potential modes, (i) collective magnetic excitation and (ii) superparamagnetic relaxation (SP). In (i) the magnetization vector performs small fluctuation around an easy direction. If these fluctuations are fast compared to the Mössbauer time scale, there will be a reduction in average magnetic hyperfine field given by [35]):

$$B_{obs} = B_0[1 - 1/2(kT/KV)] \tag{4}$$

for $KV \gg kT$. Where, B_0 is the hyperfine field of a larger particle, i.e. in the absence of fluctuation. In (ii) the magnetization vector fluctuates between the two energy minima, $\theta = 0$ and π (equation 3). For this case the superparamagnetic relaxation time is given by [36, 37]

$$\tau = \tau_0 \exp[KV/kT] \tag{5}$$

where τ_0 is a proportionality constant (10^{-10}–10^{-12}s). The temperature at which the magnetic hyperfine splitting collapses due to fast SP relaxation is called SP blocking temperature, T_B. Therefore, the observed behaviour at 300 K may be because of these two effects. But as the SP relaxation can be suppressed effectively by applying

an external magnetic field, a field of 6 kOe was applied at room temperature. Figure 5b shows the effect of this field on the Mössbauer spectra. This confirms the SP behaviour in the system. Figure 5c shows the 80 K spectrum of MF5, which clearly indicates that for this system the T_B is > 80 K (in Mössbauer time scale i.e. $5*10^{-9}$ for ^{57}Fe).

3.3 *Magnetic properties of ferrofluid*

The above fine particles were used to prepare the magnetic fluid. Long range stability was achieved by coating particles with long chain surfactant. At room temperature M-H curve shows zero remanence and coercivity (figure 6). To describe magnetization of the magnetic fluid several theoretical models are being used [38]. The simplest is the Langevin's model, where each magnetic particle is considered to be independent, and the system resembles a paramagnetic gas. The magnetization M as a function of applied field H is given by,

$$M = M_s L(\alpha),\ L(\alpha) = \coth(\alpha) - 1/\alpha,\ \alpha = mH/kT. \tag{6}$$

Applying the above function for a log-normal distribution of particles, Chantrell *et al* [39] deduced a relation to determine the mean grain diameter D_m and the standard deviation σ which is given by

$$D_m = [(18kT/\pi M_d)\{\chi_i/3\Phi M_d H_0\}^{1/2}]^{1/3} \tag{7}$$

$$\sigma = [\ln(3\chi_i H_0/\Phi M_d)^{1/2}]/3 \tag{8}$$

where, χ_i = initial susceptibility, Φ = volume fraction of particles in fluid, $1/H_0$ = point where the extrapolation of linear part of $M - 1/H$ curve crosses the $M = 0$ axis (large H). Using (7, 8) mean diameter and σ were calculated and same are given in table 1. Equations (7) and (8) are useful when there is no particle-particle interaction, because this makes a rather small correction to particle diameter, whereas there is a large correction to the standard deviation (30 to 40%) [40]. Recent studies by Hilo *et al*

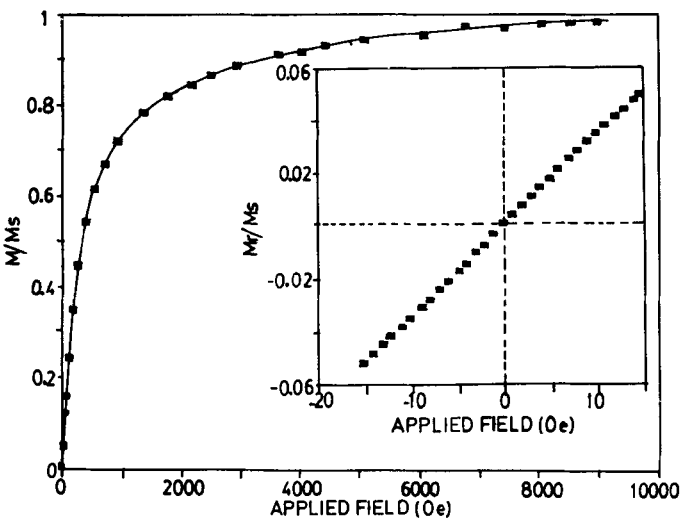

Figure 6. Isothermal magnetization as a function of applied field for MF5 fluid at 298 K. Line through the data points is calculated using equation (11). Inset: The low field data.

[41] indicate that even in most dilute system there exists a possibility of particle-particle interaction. Therefore, in our earlier study [42] we have used the method given by Shah and Mehta [43]. According to this method at low field larger particles are completely oriented while the finer particles are oriented at high field. Therefore one can find a uniform distribution extending from a minimum volume (V_{min}) to a maximum volume (V_{max}). Using the asymptotic behaviour of (6) one obtains for low field region, i.e. $mH/kT \ll 1$,

$$\bar{M} = M/M_s = x^a/3 \tag{9}$$

and for high field region, i.e. $mH/kT \gg 1$,

$$\bar{M} = M/M_s = 1 - 1/x^b \tag{10}$$

where, $x^a = M_d V_{max} H/kT$, and $x^b = M_d V_{min} H/kT$. These values of V_{max} and V_{min} can be obtained from the reduced initial susceptibility, $\chi_i = d\bar{M}/dH$ for $H < 30$ Oe, and plot of M versus $1/H$ in high field region, respectively. Using these values one can obtain the magnetization curve using the relation,

$$\bar{M} = \int_{V_{min}}^{V_{max}} L(M_d VH/kT)dV/(V_{max} - V_{min})$$
$$= kT/[M_d H(V_{max} - V_{min})]\ln\{(V_{min}/V_{max})\sinh(x^b)/\sinh(x^a)\}. \tag{11}$$

Figure 6 shows the M/M_s versus H curve for this fluid. Using the values of V_{min} and V_{max} from this result and using (11) M was calculated for each value of H and same is shown as solid line in figure 6. In the present case the values of diameters correspond to these volumes are 30 A and 107 A, respectively. The average value of these is 69 A which is in good agreement with X-ray and electron microscopy results (table 1).

Figure 7 shows the variation of dc-susceptibility with temperature. The observed behaviour can be explained by considering Néel's model [37]. For a dc-measurement the experimental time is taken to be 100 s. This gives a critical volume, V_p, defined

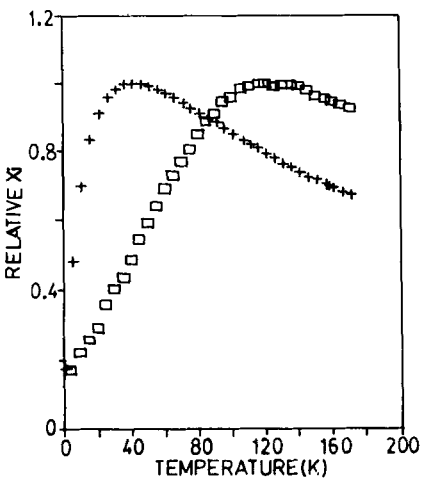

Figure 7. DC-susceptibility variation with temperature. (+) calculated using equation (15) and (□) experimental.

by [13],

$$KV_p = \ln(t_m f_0) kT_B \tag{12}$$

where, t_m is measuring time. According to Wohlfarth [44] the susceptibility for a particle with volume V is given by

$$\chi_i = M_d^2/3K, \qquad T < T_B, \text{ (Block)}$$
$$\chi_i = M_d^2 V/3kT, \quad T > T_B, \text{ (SP)} \tag{13}$$

But as we have discussed earlier, in real system there will be a distribution of particle size, i.e. distribution of T_B, therefore the mean blocking temperature, $\langle T_B \rangle$, corresponding to mean volume, V_m, within a system can be defined as [13]

$$\langle T_B \rangle = [KV_m/k \ln(t_m f_0)]. \tag{14}$$

For a non-interacting fine particle system with randomly oriented easy axes the reduced initial susceptibility, $\bar{\chi}_i (= \chi_i/M_s)$ is given by [41],

$$\bar{\chi}_i(T) = (M_d V_m/3kT) \int_0^{y_p(H,T)} y f(y) \mathrm{d}y + (M_d/3K) \int_{y_p(H,T)}^{\infty} f(y) \mathrm{d}y \tag{15}$$

where, $y = V/V_m$ and $y_p(H, T) = V_p(H, T)/V_m$. For dc-measurement, when $H \to 0$, the critical limit for SP behaviour will be $V_p(H, T) = V_p(0, T)$. If K remains invariant, the reduced critical limit for SP is $y_p(0, T) = T/T_B$. In (15), the first integral represents the contribution of SP particles, which is the main contribution to susceptibility, and second represents the contribution of blocked particles. Therefore the variation of χ_i with T will give a peak at $T = T_g$. But recently El-Hilo *et al* [41] have studied the influence of dipolar interaction between the particles on the value of T_g by considering the effects of particle interaction on the blocking temperature. They found that in the case of weakly interacting system the effective mean blocking temperature, $\langle T_{B_{eff}} \rangle$, is given by

$$\langle T_{B_{eff}} \rangle = 1/2[\langle T_B \rangle + \langle T_B \rangle \{1 + (4\xi_1 M_d^4 \ln(t_m f_0)/3K^2)\}^{1/2}] \tag{16}$$

where ξ_1 is an interaction parameter. When $\xi_1 \to 0$, $\langle T_{B_{eff}} \rangle \to \langle T_B \rangle$. Since the temperature of the peak in dc-susceptibility is directly related to $\langle T_{B_{eff}} \rangle$, i.e. mean energy barrier, T_g will occur at higher temperature, due to the dipolar interaction. This is shown in figure 7. The position of the peak was found to shift to lower temperature with dilution, but even for dilute system position of the peak does not superimpose on the curve obtained using (15) indicating that even in this case there exist a finite clustering in the system. In order to find the energy barrier distribution, i.e. blocking temperature distribution, the temperature decay of remanence measurement was carried out.

Figure 8 shows the temperature dependence of remanent magnetization. These data show the classical behaviour similar to that previously reported [41, 45]. As it is known that the remanence at any temperature gives the measure of the particle fraction which are blocked, the energy distribution can be obtained by fitting the decay curve using the expression of Tari *et al* [46]

$$M_r(T) = M_r(0) \left[\int_{T/\langle T_B \rangle}^{\infty} f(T_R) \mathrm{d}y \right] \tag{17}$$

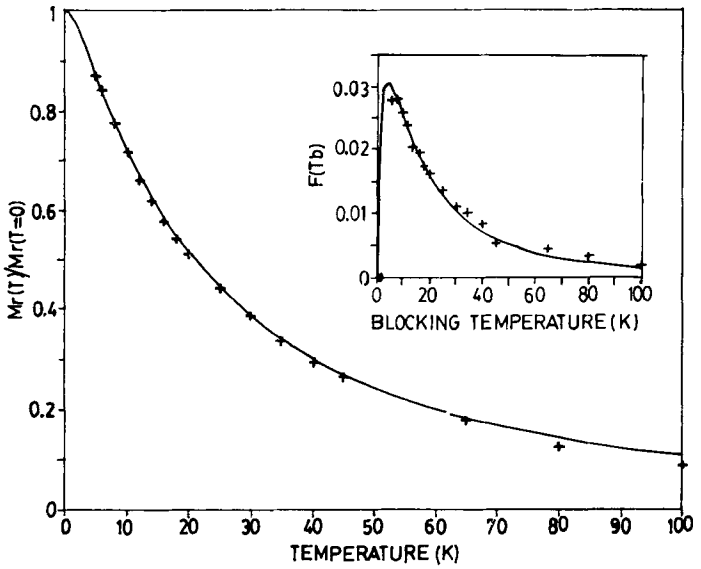

Figure 8. Temperature decay of remanence for magnetic fluid. Inset: Distribution of blocking temperature. Solid line is the theoretical fit to the data (see text).

where, $T_R = T_B/\langle T_B \rangle$ = reduced blocking temperature and $f(T_R)$ is the distribution of reduced blocking temperature. The curve in figure 8 was fitted to the solid line which was computed from equation (17) using a log-normal distribution of T_R, i.e.,

$$f(T_R) = (1/(\sigma_y T_R \sqrt{2\pi}))[\exp(-(\ln T_R)^2/2\sigma_y^2)] \tag{18}$$

The fit was achieved using only two variable parameters, $\langle T_B \rangle$ and σ_y. Here $\langle T_B \rangle$ is the temperature at which half of the total magnetic volume will exhibit blocked behaviour. The distribution parameter used were $\langle T_B \rangle = 18$ K and $\sigma_y = 1{\cdot}2$ of log-normal distribution. Since $T_B \propto KV$, and dM_r/dT is proportional to $f(T_B)$. The inset in figure 8 represents the differential of remanence data. The solid line through the data points is calculated using the above values of blocking temperature and σ_y. This value of $\langle T_B \rangle$ was used to estimate the value of anisotropy constant, K, using the relation [47],

$$KV_m = 32k\langle T_B \rangle. \tag{19}$$

Here we have used the value of $f_0 = 10^{12}\,s^{-1}$. This calculation gives the value of $K = 2{\cdot}9 \times 10^5$ erg/cm^3. According to Hilo *et al* [41] the remanence measurements are not sensitive to interaction effect, therefore the value of blocking temperature is a true value, not effective T_B. In the present system it was observed that at 4·2 K the value of $M_r/M_s = 0{\cdot}39$ and which on extrapolation to 0 K gives 0·42. This indicates that 16% (because for randomly oriented axes the value reaches 0·5 [48]) of the particle does not contribute to remanence. Similar effects were also observed by other workers [41, 45]. It is seen from figure 8 that remanence is nearly zero for $T > 115$ K, indicating that for a time scale of 100 s the system becomes SP above this temperature. For such a system equation (11) can be applied and when M/M_s versus H/T is plotted one observes the superposition of curves for different temperatures. Figure 9 shows the H/T superposition for two different temperature. The solid line through the data

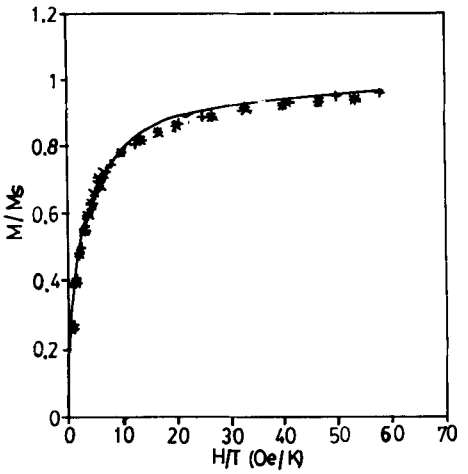

Figure 9. H/T superposition for MF5 fluid. + 121 K, * 145 K.

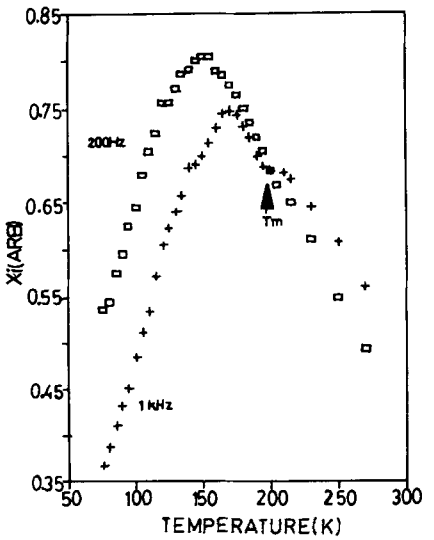

Figure 10. Variation of ac-susceptibility with temperature.

point is calculated using (11). The observed agreement and superposition of curves clearly suggests that the system is SP for $T > 120$ K, which is in accordance with the observed zero remanence and coercivity and SP behaviour in Mössbauer for the particles and the fluid.

Figure 10 shows the ac-susceptibility measurements for two different frequencies. The ac-susceptibility measures only a reversible part of magnetization curve. Based on our earlier discussion it is certain that the observed peak is connected with the thermally activated reversal process of the magnetic moments of SP particles, i.e. blocking temperature. At T_B the relaxation time of thermal activation of grain volume becomes equal to the reciprocal of measuring frequency. Therefore higher the frequency the T_B will be higher, this is observed in the present case (figure 10). The change in the behaviour around 200 K is due to the change in the state, i.e. solid to liquid. Therefore the system exhibits two relaxation times in magnetization dynamics;

(i) t_N, for Néel process and (ii) t_B, Brownian motion. Below the melting temperature t_B becomes infinity therefore the main contribution to the relaxation mechanism will be Neel, while above the melting point it depends upon the magnitude of the individual. Both these relaxation times are given by,

$$t_N = t_0 \exp(KV/kT),$$
$$t_B = 3V'\eta/kT. \tag{20}$$

where, V' = hydrodynamic volume, η = viscosity of fluid. From (20) it can be seen that the relaxation domain for t_N is very large compared to t_B, i.e. t_N varies with particle size from 10^{-12} to 10^{12}s while t_B changes only by one order, 10^{-5} to 10^{-6}s. Because of these one can use the frequency dependence of ac-susceptibility technique (above melting point) for the characterization of magnetic fluid, i.e. agglomeration or clustering.

Conclusion

The present study reveals that
(1) With 50% substitution of Mn it is possible to synthesize ultra-fine particles having average diameter of 70 A. (2) The value of saturation magnetization of uncoated particles are affected by surface pinning effect. (3) Sterically stabilized colloidal dispersion of these particles gives a stable magnetic fluid of 350 G. (4) This system was found to obey log-normal particle size distribution. (5) Temperature decay of remanence gives the anisotropy value of $2{\cdot}9 \times 10^5$ erg/cc. (6) System behaves as superparamagnet above 80 K.

Acknowledgements

The authors are thankful to Drs S W Charles and Steen Mørup for providing experimental facilities and valuable discussion.

References

[1] J Smit and H P J Wijn, "*Ferrites*" (Eindhoven, Philips, 1959)
[2] J B Goodenough, *Prog. Solid State Chem.*, **5**, 145 (1971)
[3] C P Poole and H A Farach, *Z. Phys.*, **B47**, 55 (1982)
[4] J Schuele and V D Deetscreek, *J. Appl. Phys.*, **32**, 235S (1961)
[5] T Sato, C Kuroda, M Saito and M Sugihara, *Proc. Int. Conf. on ferrite.*, Tyoto, 1970 (University Park Press, Tokyo, 1972) 72
[6] R E Vadenberghe, R Vanleerberghe and Robbrecht, *J. Magn. Magn. Mater.*, **15–18**, 1117 (1980)
[7] T Sato, *IEEE Trans. Magn.*, **MAG-6**, 795 (1970)
[8] M Kiyama, *Bull. Chem. Soc. Jpn.*, **951**, 134 (1978)
[9] E Matijevic, *MRS bulletin*, **XIV**, 19 (1989)
[10] M Ozaki, *MRS bulletin*, **XIV**, 35 (1989)
[11] M P Scharrock and R E Bodnar, *J. Appl. Phys.*, **57**, 3919 (1989)
[12] R E Rosensweig, *U.S. Patent* **3**, 917 538 (1975)
[13] C P Bean and J D Livingston, *J. Appl. Phys.*, **305**, 120S (1959)
[14] R F Penoyer and M W Shafer, *J. Appl. Phys.*, **30**, 315S (1959)
[15] R E Rosensweig, *Adv. Electron. Electron. Phys.*, **48**, 103 (1979)
[16] R V Mehta, *J. Sci. Ind. Res.*, **44**, 500 (1985)

[17] S W Charles and J Popplewell, *Endeavour*, **6**, 153 (1982)
[18] M Zahn and K E Shanton, *IEEE Trans. Magn.*, **MAG-16**, 387 (1980)
[19] S W Charles and R E Rosensweig, *J. Magn. Magn. Mater.*, **39**, 190 (1983)
[20] S Kamiyama and R E Rosensweig, *J. Magn. Magn. Mater.*, **65**, 401 (1987)
[21] E Blums, R Ozols and R E Rosensweig, *J. Magn. Magn. Mater.*, **85**, 303 (1990)
[22] R K Bhatt, P M Trivedi, G M Sutariya, R V Upadhyay and R V Mehta, *Indian J. Pure Appl. Phys.*, **33**, 113 (1993)
[23] E L Resler and R E Rosensweig, *AIAA J.*, **2**, 1418 (1964)
[24] G M Sutariya, R V Upadhyay and R V Mehta, *J. Colloid. Interface Sci.*, **155**, 152 (1993)
[25] T Miyahara and K Wawakauri, *IEEE Trans. Magn.*, **MAG-23**, 2877 (1987)
[26] S Komarneni, E Fregau, E Breval and R Roy, *J. Am. Ceram. Soc.*, **71**, C-26 (1988)
[27] G Xiao and C L Chien, *J. Appl. Phys.*, **61**, 3308 (1987)
[28] C F Kernizan, K H Klabunde, C M Sorensen and G C Hadjipanayis, *J. Appl. Phys.*, **67**, 5897 (1990)
[29] C Hayashi, *J. Vac. Sci. Technol.*, **A5**, 1375 (1987)
[30] V Pillai, P Kumar and D O Shah, *J. Magn. Magn. Mater.*, **116**, L299 (1992)
[31] F Soffge and Schmidbauer, *J. Magn. Magn. Mater.*, **24**, 54 (1981)
[32] J B Goodenough, *Magnetism and Chemical Bond* (Wiley, New York, 1963)
[33] M Robbins, *J. Phys. Chem. Solid*, **26**, 831 (1965)
[34] K O'Grady and A Bradbury, *J. Magn. Magn. Mater.*, **39**, 91 (1984)
[35] S Mørup, J A Dumesic and H Topsøe, "*Application of Mössbauer Spectroscopy*" Edited by R L Cohen (New York, Academic Press, 1980) 1
[36] S Mørup, H Topsøe and B S Clausen, *Phys. Scr.*, **25**, 713 (1982)
[37] L Neél, *Ann. Geophys.*, **5**, 99 (1949)
[38] M I Shliomis, A F Pshenichnikov, K I Morozov and I Yu Shurubor, *J. Magn. Magn. Mater.*, **85**, 40 (1990)
[39] R W Chantrell, J Popplewell and S W Charles, *IEEE Trans. Magn.*, **MAG-14**, 975 (1978)
[40] A Bradbury, S Menear, K O'Grady and R W Chantrell, *IEEE Trans. Magn.* **MAG-20**, 1846 (1984)
[41] M El-Hilo, K O'Grady and R W Chantrell, *J. Magn. Magn. Mater.*, **114**, 295, 307 (1992)
[42] R V Upadhyay, G M Sutariya and R V Mehta, *J. Magn. Magn. Mater.*, **123**, 262 (1993)
[43] H S Shah and R V Mehta, *Indian J. Pure Appl. Phys.*, **11**, 537 (1973)
[44] E P Wohlfarth, *Phys. Lett.*, **A70**, 489 (1989)
[45] R W Chantrell, M El-Hilo and K O'Grady, *IEEE Trans. Magn.*, **MAG-27**, 3570 (1991)
[46] A Tari, R W Chantrell, S W Charles and J Popplewell, *Physica* **B97**, 599 (1984)
[47] D P E Dickson, N M K Reid, C A Hunt, H D Williams, M El-Hilo and K O'Grady, (In Press) (1993)
[48] E C Stoner and E P Wahlfarth, *Philos. Trans. R. Soc., London*, ser **A240**, 599 (1948)